Acta Crystallographica Section D
Biological Crystallography
ISSN 0907-4449

Crystallization and preliminary X-ray diffraction studies of a mosquito-larvicidal toxin from *Bacillus thuringiensis* subsp. *israelensis*

Panadda Boonserm,[a]*† David J. Ellar[a] and Jade Li[b]

[a]Department of Biochemistry, University of Cambridge, Tennis Court Road, Cambridge CB2 1GA, England, and [b]Medical Research Council Laboratory of Molecular Biology, Hills Road, Cambridge CB2 2QH, England

† Present address: Institute of Molecular Biology and Genetics, Mahidol University, Salaya Campus, Nakornpathom 73170, Thailand.

Correspondence e-mail: mbpbs@mahidol.ac.th

Received 10 October 2002
Accepted 16 January 2003

The Cry4B δ-endotoxin from *Bacillus thuringiensis* subsp. *israelensis* is specifically toxic to mosquito larvae. For a better understanding of the mechanism of toxicity, chymotrypsin-activated Cry4B toxin (68 kDa) has been purified and crystallized in sodium bromide at neutral pH. The well formed crystals belong to the rhombohedral space group *R*32, with unit-cell parameters $a = b = 185.82$, $c = 187.93$ Å, and diffracted X-rays to 1.75 Å resolution. The asymmetric unit contains one toxin molecule and 74% solvent content, as shown by molecular replacement from a composite model of the homologous Cry3A and Cry1Aa. The purified protein and crystals both possessed mosquitocidal activity.

1. Introduction

The spore-forming bacterium *Bacillus thuringiensis* (Bt) produces highly specific insecticidal crystal proteins (ICPs; Knowles, 1994) which have been classified into two main families, Cry and Cyt toxins, based on amino-acid sequence identity (Crickmore *et al.*, 1998). Most ICPs are synthesized as inactive protoxins which, upon ingestion by the insect, are solubilized in the insect midgut and activated by gut proteases. The activated toxin binds to a specific receptor on the midgut epithelial cells and inserts into the membrane, creating transmembrane leakage pores that cause cell swelling and disruption by colloid osmotic lysis (Knowles & Ellar, 1987).

Crystal structures have been elucidated for Cry toxins with specificities against coleopteran (Li *et al.*, 1991; Galitsky *et al.*, 2001), lepidopteran (Grochulski *et al.*, 1995; Derbyshire *et al.*, 2001; Li *et al.*, 2001) and lepidopteran-dipteran insects (Morse *et al.*, 2001). These structures differ significantly in detail but show a common fold consisting of an α-helical bundle (domain I), a three β-sheet prism (domain II) and a β-sandwich (domain III). The functional role inferred from the domain conformation and the experimental evidence both indicate that domain I is responsible for pore formation (Ahmad & Ellar, 1990; Li *et al.*, 1991; Wu & Aronson, 1992; Grochulski *et al.*, 1995; Schwartz *et al.*, 1997) and domain II is involved in receptor and membrane binding (Ge *et al.*, 1989; Schnepf *et al.*, 1990; Smith & Ellar, 1994; Smedley & Ellar, 1996; Morse *et al.*, 2001), while domain III serves to protect the protease-resistant core from further proteolysis (Li *et al.*, 1991) and participates in specificity determination (Lee *et al.*, 1995; de Maagd *et al.*, 1996; Burton *et al.*, 1999) and regulation of ion-channel activity (Chen *et al.*, 1993; Wolfersberger *et al.*, 1996; Schwartz *et al.*, 1997). As yet, no structural information is available for Cry toxins with specific toxicities towards dipteran insects (*e.g.* mosquitoes).

B. thuringiensis subsp. *israelensis* (Bti) is specifically and highly toxic towards the larvae of *Aedes* and *Anopheles* mosquitoes, the transmitters of dengue fever and malaria (Roberts, 2002), and is widely used as an insecticide (Höfte & Whiteley, 1989). One of the four major toxins produced by Bti is Cry4B. Cry4B is synthesized as a 130 kDa protoxin and is processed by mosquito-gut proteases to the active toxin (Angsuthanasombat *et al.*, 1991). Amino-acid sequence alignment among Cry toxins reveals that Cry4B also contains the five conserved sequence blocks (Höfte & Whiteley, 1989; Hodgman & Ellar, 1990) seen to form the structural core in other Cry toxins (Li *et al.*, 1991; Grochulski *et al.*, 1995). This suggests that the structure of Cry4B will be based on a similar fold.

The mechanism of mosquito-specific toxicities is not well understood at present. The crystal structure of the highly specific mosquitocidal Cry4B will provide an essential framework for mutagenic and biophysical investigations of the mechanisms and may facilitate the genetic engineering of improved toxins. Here, we describe the crystallization and preliminary crystallographic characterization of the activated fragment of Cry4B toxin.

2. Materials and methods

2.1. Inclusion, purification and solubilization

The Cry4B protoxin was expressed as inclusions in sporulating cells of Bti IPS78/11

reduced-protease strain (E41-3) containing plasmid Cam135 (Angsuthanasombat *et al.*, 1991). The inclusions and spores released into the medium at the end of sporulation were collected and washed three times with buffer *A* [20 m*M* Tris–HCl pH 7.4, 10 m*M* KCl, 5 m*M* EDTA, 0.5 m*M* benzamidine, 0.5 m*M* phenyl methylsulfonyl fluoride (PMSF)] by centrifugation for 15 min at 3000*g*, 277 K. The inclusions were then isolated from spores by differential ultracentrifugation (Thomas & Ellar, 1983*a*) as a major band at the interface between sucrose concentrations of 2.1 and 2.4 *M*. These purified crystalline inclusions were solubilized in 50 m*M* Na_2CO_3 pH 10.5, 100 m*M* NaBr, 5 m*M* dithiothreitol (DTT), 5 m*M* benzamidine, 2 m*M* tosyl-lysine chloromethyl ketone (TLCK), 1 m*M* EDTA at 310 K for 1 h. Insoluble material was sedimented by centrifugation for 15 min at 3000*g*.

2.2. Proteolytic activation

Solubilized 130 kDa protoxin was incubated with TLCK-treated chymotrypsin [Sigma; 1:5(*w*/*w*) enzyme:protoxin] at 310 K for 1 h; the reaction was then stopped by adding 1 m*M* tosyl-phenylalanine chloromethyl ketone (TPCK). In parallel experiments, the protoxin was incubated with trypsin and the reaction was stopped using TLCK. The proteolytic products were examined by SDS–PAGE and tested for *in vitro* cytotoxicity against mosquito cells (Thomas & Ellar, 1983*b*).

2.3. Protein purification by FPLC

Chymotrypsin-activated Cry4B was concentrated by ultrafiltration using a Centriprep column (Amicon) with a 30 kDa cutoff at 277 K. This was loaded onto a Superose 12 column (Pharmacia), which was connected to a Pharmacia FPLC apparatus and previously equilibrated with 50 m*M* Na_2CO_3 pH 10.5, 100 m*M* NaBr, 2 m*M* DTT, 2 m*M* benzamidine, 1 m*M* EDTA. Activated Cry4B was eluted from the column at a flow rate of 0.5 ml min^{-1} in the peak at 12–14 ml, which is about 50% of the column bed volume (24 ml) and corresponds to the eluted fractions of the protein marker BSA (67 kDa). Fractions across this peak were pooled and concentrated to 5–8 mg ml^{-1} by ultrafiltration as described previously.

2.4. Crystallization and data collection

Crystals were grown by vapour diffusion in hanging drops. 2–4 µl of protein at 5–8 mg ml^{-1} was mixed with reservoir solution containing 100 m*M* Tris–HOAc pH 7–8, 0.4–0.6 *M* NaBr in volume ratios of 1:1, 2:1 or 2.5:1 and equilibrated against 1 ml of the reservoir at 295 K. Crystals appeared after a period of 2 d to three weeks and grew to their maximum size in three months. Prior to data collection, the crystal was incubated for at least 10 min in a stabilizing buffer containing 100 m*M* Tris–HOAc pH 7.0, 0.6 *M* NaBr. The crystal was transferred in 20 µl of the stabilizing buffer to a glass depression slide. The crystal was equilibrated in steps containing increasing amounts of cryoprotectant by replacing half the buffer around the crystal with a cryoprotecting solution consisting of 20% 2-methyl-2,4-pentanediol (MPD) and 10% polyethylene glycol (PEG) 400 dissolved in the stabilizing buffer and gently mixing by using a Gilson pipette. Finally, the crystal was placed in the cryoprotection solution, mounted in a Cryoloop (Hampton Research) and flash-frozen by exposure to N_2 vapour at 100 K.

X-ray data were collected using either a rotating-anode source and a 345 mm MAR image-plate detector (MAR Research) or using the synchrotron source at Station 14.2, Synchrotron Radiation Source Daresbury Laboratory (Warrington, England) with 0.978 Å wavelength and a Quantum IV CCD detector. Data were processed using *MOSFLM* (Leslie, 1992) and other programs from the *CCP*4 suite (Collaborative Computational Project, Number 4, 1994). Molecular replacement was carried out using *AMoRe* (Navaza, 1994).

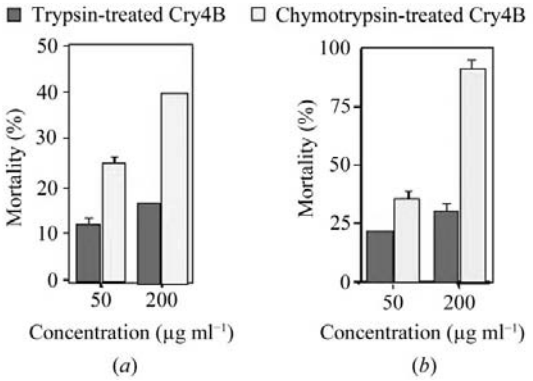

Figure 1
Percentage mortality of *Aedes albopictus* (*a*) and *Anopheles gambiae* (*b*) after exposure to trypsin- and chymotrypsin-activated Cry4B toxin at concentrations of 50 and 200 µg ml^{-1}. The percentage of dead cells and error bars are based on three separate experiments. The percentage mortality in control cells incubated with buffer containing only each enzyme has been subtracted in the figure.

3. Results and discussion

3.1. Protein activation and purification

Angsuthanasombat *et al.* (1991) reported that upon treatment with *Aedes aegypti* mosquito-larval gut extract or with trypsin, the 130 kDa Cry4B protoxin was readily converted to polypeptides of 60–70 kDa, which corresponded to the molecular weight of the three-domain toxin, and that these were further cleaved into two fragments of 46–48 and 16–18 kDa. Whereas the N-terminal sequence of the 16–18 kDa fragment was identical to that of the 60–70 kDa polypeptide, the N-terminal sequence of the 46–48 kDa fragment was mapped to a cleavage site in the loop connecting helices 5 and 6 by alignment with the Cry3A structure (Hodgman & Ellar, 1990; Li *et al.*, 1991). In this work, incubation of the solubilized Cry4B protoxin with chymotrypsin [1:5(*w*/*w*) enzyme:toxin] at 310 K for 1 h resulted in a single major polypeptide of 68 kDa. N-terminal sequencing confirmed that it was N-terminally cleaved by chymotrypsin between Tyr33 and Gly34; alignment with Cry3Aa placed this cleavage site before the beginning of helix 1 in domain I. The smaller fragments generated in minor amounts were most likely to have arised from trypsin contamination, as suggested by the effects of specific protease inhibitors.

Chymotrypsin-treated Cry4B was tested for cytotoxicity against mosquito cell lines (Thomas & Ellar, 1983*b*) in comparison with trypsin-treated Cry4B. It was found that the Cry4B activated with chymotrypsin was significantly more toxic towards *Aedes albopictus* and *Anopheles gambiae* cells than the trypsin-activated Cry4B (Fig. 1). These results indicate that chymotrypsin does not cleave the portions of the protein that are necessary for biological activity against mosquito cells, whereas the toxicity is reduced by the treatment with trypsin.

The chymotrypsin-activated Cry4B was purified as a monomer by gel filtration (see §2.3).

3.2. Crystallization and cryoprotection

Since Cry4B solubilized at alkaline pH is known to become less soluble towards neutral pH, the initial approach to promote crystal formation was to lower the pH by adding 100 m*M* Tris–HCl pH 7–9 to the purified protein at pH 10.5. This was combined with the addition of other preci-

pitants. Thin plates were occasionally observed in 10% PEG 4000, 100 m*M* Tris–HCl pH 8.5 and pH 9.0. Clustered needles were found in two conditions containing 100 m*M* Tris–HCl pH 9.0, 0.25 *M* Li_2SO_4 and 100 m*M* Tris–HCl pH 9–10, 0.25 *M* K_2HPO_4. Single crystals of 5–10 µm in size appeared after three weeks in 100 m*M* Tris–HCl pH 9.0, 0.25 *M* sodium formate. All these crystals were too small or disordered for X-ray diffraction studies (data not shown).

The crystal form used for data collection was first observed after three months from a condition containing 100 m*M* Tris–HCl pH 9.0, 0.5 *M* NaBr. However, nucleation under these conditions was erratic and growth was imperceptibly slow, making optimization difficult. By adding 2%(*v*/*v*) 2-methyl-2,4-pentanediol (MPD) to duplicate drops containing 0.5 *M* NaBr at pH 7.5–9.0, the threshold for nucleation was lowered so that small crystals appeared in every drop and it then became clear that lower pH was correlated with larger crystal size. Therefore, omitting MPD, the reservoir buffer was changed to Tris–HOAc in order to gradually acidify the protein drop through vapour diffusion. Simultaneously lowering the pH and increasing the NaBr concentration resulted in larger well formed crystals. Under the optimal conditions 100 m*M* Tris–HOAc pH 7–8, 0.4–0.6 *M* NaBr, a maximal size of 0.5–0.8 mm was reached over a period of three weeks to three months. Increasing the protein:precipitant ratio from 1:1 to 2:1 or 2.5:1 accelerated the growth so that maximum size was reached in two weeks. These crystals were typically rhomboids or trigonal pyramids with sharp edges (Fig. 2). They were highly birefringent and extinguished polarized light sharply when rotated.

The tendency of MPD to increase supersaturation (see §3.2) was exploited in the cryoprotection. Cryobuffers incorporating 25–30% glycerol prevented ice formation but caused disorder and high mosaicity, as indicated by the absence of diffraction beyond ∼3.5 Å and fuzziness of the spots. Using 30% MPD extended the resolution to 2.4 Å, but caused the crystal to crack. 25% PEG 400 was intermediate between the glycerol and MPD in its effectiveness in stabilizing the crystalline order and caused no cracking. Optimal cryoprotection was achieved by combining 20% MPD with 10% PEG 400, resulting in a resolution of 2.2 Å. By introducing cryoprotectants into the stabilizing buffer around the crystal in a stepwise fashion (see §2.4), the mosaicity was as low as 0.35°.

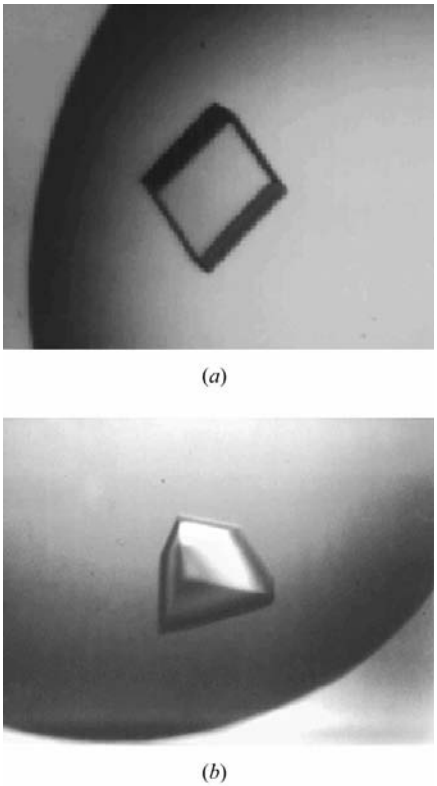

Figure 2
Typical crystals of mosquitocidal Cry4B toxin. The dimensions of the crystals are (*a*) 0.65 × 0.65 mm and (*b*) 0.75 × 0.75 mm.

3.3. Crystallographic characterization

Using a synchrotron source, a complete data set with high redundancy was collected from a frozen crystal (see §2.4) to 1.75 Å resolution, with a low-resolution pass to 2.7 Å for scaling. The crystal showed no detectable radiation damage. Data statistics are summarized in Table 1. The crystals were shown by molecular replacement to contain one toxin molecule and ∼74% solvent in the asymmetric unit, corresponding to a V_M of 4.8 $Å^3$ Da^{-1} (Matthews, 1968).

Structures of two Cry toxins, Cry3A (PDB code 1dlc; Li *et al.*, 1991) and Cry1Aa (PDB code 1ciy; Grochulski *et al.*, 1995) were available as molecular-replacement models. They show only low homology with Cry4B, with sequence identities of 20 and 23%, respectively. Using either structure alone the molecular orientation could not be determined with confidence, as the rotation peaks found by *AMoRe* (Navaza, 1994) showed at best a ∼5% amplitude correlation with the data. To reinforce the similarities between the models and target, a composite search model was constructed by least-squares superposition (calculated using the program *LSQMAN*; Kleywegt, 1996) of Cry3A and Cry1Aa over the five conserved sequence blocks that are present in almost all toxins of the family (Höfte & Whiteley, 1989). A molecular-replacement solution was readily obtained which had a 31% correlation with the data after rigid-body refinement. The significant and yet relatively low correlation indicates that the Cry4B structure should share the same fold as the other Cry toxins and yet show significant differences with the known structures. In a bioassay using mechanically fragmented Cry4B crystals and *Aedes aegypti* larvae, the crystals were found to possess larvicidal toxicity (Boonserm & Ellar, unpublished). Therefore, determining the structure of Cry4B promises to reveal the range of structural variations that are pertinent to its distinct insecticidal specificities.

Table 1
Statistics of X-ray diffraction data.

Values in parentheses are for the last resolution shell.

Unit-cell parameters (Å)	
$a = b$	185.82
c	187.93
Resolution (Å)	1.75 (1.84–1.75)
Mosaicity (°)	0.30
Unique reflections	124540 (18032)
Completeness (%)	100 (100)
Multiplicity	9.7 (8.5)
R_{merge}† (%)	6.6 (35.1)
Average $I/\sigma(I)$	24.1 (5.1)

† R_{merge} (%) = $(\sum|I_i - \langle I\rangle|/\sum I_i) \times 100$, where I_i is an individual intensity observation, $\langle I\rangle$ is the mean intensity of that reflection and the summation is over all reflections.

We thank Dr Neil Crickmore for providing the plasmid construct in this study and Daresbury Laboratory for use of the Synchrotron Radiation Source. We acknowledge financial support from the Royal Thai Government.

References

Ahmad, W. & Ellar, D. J. (1990). *FEMS Microbiol. Lett.* **68**, 97–104.
Angsuthanasombat, C., Crickmore, N. & Ellar, D. J. (1991). *FEMS Microbiol. Lett.* **67**, 273–276.
Burton, S. L., Ellar, D. J., Li, J. & Derbyshire, D. J. (1999). *J. Mol. Biol.* **287**, 1011–1022.
Chen, X. J., Lee, M. K. & Dean, D. H. (1993). *Proc. Natl Acad. Sci. USA*, **90**, 9041–9045.
Collaborative Computational Project, Number 4 (1994). *Acta Cryst.* D**50**, 760–763.
Crickmore, N., Zeigler, D. R., Feitelson, J., Schnepf, E., Van Rie, J., Lereclus, D., Baum, J. & Dean, D. H. (1998). *Microbiol. Mol. Biol. Rev.* **62**, 807–813.
Derbyshire, D. J., Ellar, D. J. & Li, J. (2001). *Acta Cryst.* D**57**, 1938–1944.
Galitsky, N., Cody, V., Wojtczak, A., Ghosh, D., Luft, J. R., Pangborn, W. & English, L. (2001). *Acta Cryst.* D**57**, 1101–1109.
Ge, A. Z., Shivarova, N. I. & Dean, D. H. (1989). *Proc. Natl Acad. Sci. USA*, **86**, 4037–4041.

Grochulski, P., Masson, L., Borisova, S., Pusztai-carey, M., Schwartz, J. L., Brousseau, R. & Cygler, M. (1995). *J. Mol. Biol.* **254**, 447–464.
Hodgman, T. C. & Ellar, D. J. (1990). *DNA Seq.* **1**, 97–106.
Höfte, H. & Whiteley, H. R. (1989). *Microbiol Rev.* **53**, 242–255.
Kleywegt, G. J. (1996). *Acta Cryst.* D**52**, 842–857.
Knowles, B. H. (1994). *Adv. Insect Physiol.* **24**, 275–308.
Knowles, B. H. & Ellar, D. J. (1987). *Biochim. Biophys. Acta*, **924**, 509–518.
Lee, M. K., Young, B. A. & Dean, D. H. (1995). *Biochem. Biophys. Res. Commun.* **216**, 306–312.
Leslie, A. G. W. (1992). *Jnt CCP4/ESF–EACMB Newsl. Protein Crystallogr.* **26**.
Li, J., Carroll, J. & Ellar, D. J. (1991). *Nature (London)*, **353**, 815–821.
Li, J., Derbyshire, D. J., Promdonkoy, B. & Ellar, D. J. (2001). *Biochem Soc Trans.* **29**, 571–577.
Maagd, R. A. de, van der Klei, H., Bakker, P. L., Stiekema, W. J. & Bosch, D. (1996). *Appl. Env. Microbiol.* **62**, 2753–2757.
Matthews, B. W. (1968). *J. Mol. Biol.* **33**, 491–497.
Morse, R. J., Yamamoto, T. & Stroud, R. M. (2001). *Structure*, **9**, 409–417.
Navaza, J. (1994). *Acta Cryst.* A**50**, 157–163.
Roberts, L. (2002). *Science*, **298**, 82–83.
Schnepf, H. E., Tomczak, K., Ortega, J. P. & Whiteley, H. R. (1990). *J. Biol. Chem.* **265**, 20923–20930.
Schwartz, J. L., Potvin, L., Chen, X. J., Brousseau, R., Laprade, R. & Dean, D. H. (1997). *Appl. Environ. Microbiol.* **63**, 3978–3984.
Smedley, P. D. & Ellar, D. J. (1996). *Microbiology*, **142**, 1617–1624.
Smith, G. P. & Ellar, D. J. (1994). *Biochem. J.* **302**, 611–616.
Thomas, W. E. & Ellar, D. J. (1983*a*). *J. Cell Sci.* **60**, 181–197.
Thomas, W. E. & Ellar, D. J. (1983*b*). *FEBS Lett.* **154**, 362–368.
Wolfersberger, M. G., Chen, X. J. & Dean, D. H. (1996). *Appl. Environ. Microbiol.* **62**, 279–282.
Wu, D. & Aronson, A. I. (1992). *J. Biol. Chem.* **267**, 2311–2317.